



Citation for published version:

Niida, Y, Takashina, K, Fujiwara, A, Fujisawa, T & Hirayama, Y 2009, 'Spin splitting of upper electron subbands in a SiO₂/Si(100)/SiO₂ quantum well with in-plane magnetic field', Applied Physics Letters, vol. 94, no. 14, 142101. <https://doi.org/10.1063/1.3105987>

DOI:

[10.1063/1.3105987](https://doi.org/10.1063/1.3105987)

Publication date:

2009

[Link to publication](#)

©2009 American Institute of Physics. This article may be downloaded for personal use only. Any other use requires prior permission of the author and the American Institute of Physics.

The following article appeared in Niida, Y., Takashina, K., Fujiwara, A., Fujisawa, T. and Hirayama, Y., 2009. Spin splitting of upper electron subbands in a SiO₂/Si(100)/SiO₂ quantum well with in-plane magnetic field. Applied Physics Letters, 94 (14), 142101, and may be found at <http://dx.doi.org/10.1063/1.3105987>.

University of Bath

General rights

Copyright and moral rights for the publications made accessible in the public portal are retained by the authors and/or other copyright owners and it is a condition of accessing publications that users recognise and abide by the legal requirements associated with these rights.

Take down policy

If you believe that this document breaches copyright please contact us providing details, and we will remove access to the work immediately and investigate your claim.

Spin splitting of upper electron subbands in a SiO₂/Si(100)/SiO₂ quantum well with in-plane magnetic field

Y. Niida,^{1,2,a)} K. Takashina,¹ A. Fujiwara,¹ T. Fujisawa,¹ and Y. Hirayama^{2,b)}

¹NTT Basic Research Laboratories, NTT Corporation, 3-1 Morinosato-Wakamiya, Atsugi, Kanagawa 243-0198, Japan

²Department of Physics, Tohoku University, 6-3 Aramaki Aza Aoba, Aoba-ku, Sendai, Miyagi 980-0845, Japan

(Received 13 October 2008; accepted 5 March 2009; published online 6 April 2009)

We observe a lifting of the twofold spin degeneracy of conduction-band electrons in an upper-valley subband with in-plane magnetic field in a SiO₂/Si(100)/SiO₂ quantum well, which is manifest in a splitting of a feature in the conductivity accompanying the occupation of the upper-valley subband. The splitting increases in proportion to the in-plane magnetic field, allowing the product of the effective g -factor and effective mass g^*m^* to be obtained. The value remains constant over wide ranges of valley splitting, total electron density, and potential bias. © 2009 American Institute of Physics. [DOI: 10.1063/1.3105987]

Besides the in-plane motion of electrons, the spin degree of freedom plays pivotal roles in the physics of two-dimensional (2D) electron systems. Fundamental phenomena, such as the metal-insulator transition and inelastic scattering, are crucially dependent on electronic spin.^{1,2} The manipulation of spin is also required for spintronic devices and a number of schemes proposed for quantum information processing.³⁻⁵ It is therefore vital to be able to measure, understand, and control spin splitting, which is the energy separation between states of opposite spin.

Here, we examine the Zeeman spin splitting of electrons in a SiO₂/Si/SiO₂ quantum well formed by fabricating a metal-oxide-semiconductor field-effect transistor (MOSFET) on a thin silicon-on-insulator (SOI) substrate. Since this structure forms the basis of much modern-day silicon nanotechnology and physics research, such basic characterization is important.

In transport measurements on Si, the Zeeman splitting has been analyzed through Shubnikov–de Haas (SdH) oscillations⁶ and magnetocapacitance measurements⁷ under magnetic field applied perpendicular to, or tilted against the 2D plane. The perpendicular magnetic field, however, affects the in-plane motion of electrons. Furthermore, Landau quantization and many body interactions are found to give rise to complicated phenomena in SiO₂/Si/SiO₂ quantum wells, which restricts the use of these techniques to a limited range of electrical bias.⁸ When only an in-plane magnetic field (B_{\parallel}) is applied so that the in-plane motion of the electrons remains relatively unaffected, the Zeeman splitting can be obtained by resistance saturation at a critical field due to full spin polarization.⁹ However, this method can only be applied to low electron densities, where full spin polarization can be achieved with accessible magnetic field strength.

In this letter, we show that spin splitting can be detected as alterations to the resistivity at the onset of the occupation of upper subbands. This allows us to extract the product of the g -factor and effective mass at higher electron densities

and without the use of a perpendicular component of magnetic field.

In silicon-based 2D systems with (100) orientation, the anisotropy of effective mass and quantum confinement lift the sixfold valley degeneracy present in the bulk to twofold and fourfold degenerate valleys, such that only the twofold degenerate valleys of lowest energy are occupied [Fig. 1(a)]. Recently, the energy splitting of the twofold states (valley splitting) was shown to be observable as features in the conductance without magnetic field and that it can be manipulated through the potential asymmetry in a SiO₂/Si/SiO₂ quantum well [Figs. 1(c) and 1(d)].¹⁰ Here, we examine the effect of B_{\parallel} on the upper-valley subband. Unlike spatially distinct confinement subbands, valley splitting is found not to depend on the in-plane field,¹¹ which opens up the possibility of isolating the effects of spin.

The sample consisted of a MOSFET fabricated on a SOI substrate as depicted in Fig. 1(b). The buried oxide (BOX)

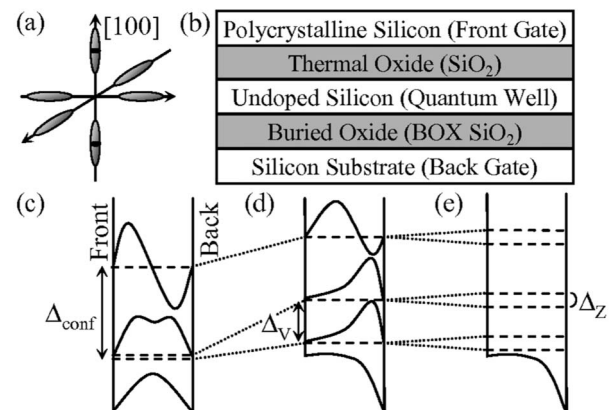


FIG. 1. (a) Fermi surfaces of electrons in bulk Si. Only the two out-of-plane valleys are occupied in our 2D system. (b) Sample structure. (c) Wave functions of the ground and upper confinement subbands in a symmetrical potential. Δ_{conf} is the difference in confinement energy of the two subbands. (d) Energy levels of the valley-split ground state and upper confinement state in an asymmetrical potential. The valley-splitting energy Δ_v is increased by the asymmetrical bias. (e) Energy levels of these states separated by the Zeeman splitting Δ_z in an in-plane magnetic field.

^{a)}Electronic mail: y-niida@mail.tains.tohoku.ac.jp.

^{b)}Also at ERATO Nuclear Spin Electronics Project, 468-15 Aramaki Aza Aoba, Aoba-ku, Sendai, Miyagi 980-0845, Japan.

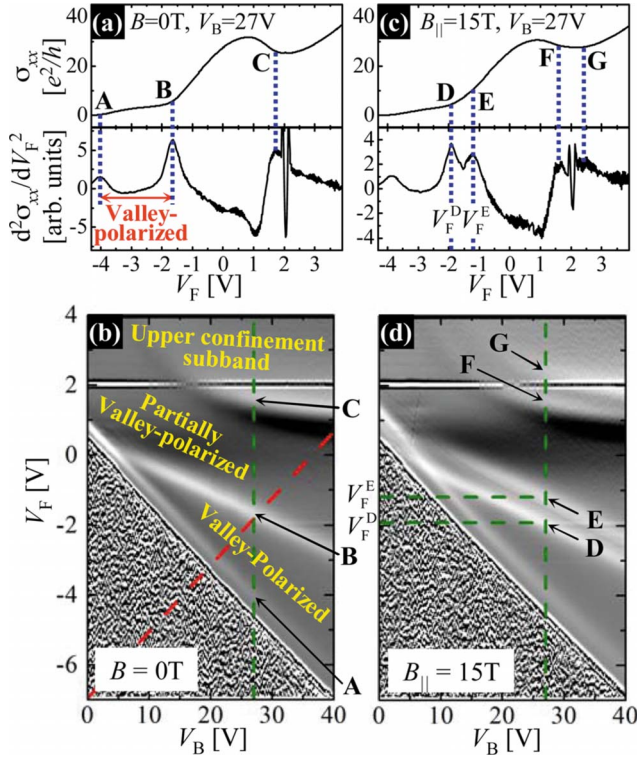


FIG. 2. (Color online) σ_{xx} and $d^2\sigma_{xx}/dV_F^2$ at $V_B=27$ V, 1.5 K, without magnetic field (a) and with $B_{\parallel}=15$ T (c). (b) and (d) are grayscale plots of $d^2\sigma_{xx}/dV_F^2$ at $B_{\parallel}=0$ T and $B_{\parallel}=15$ T, respectively, and green dashed lines mark $V_B=27$ V, $V_F=V_F^D$, and $V_F=V_F^E$. Arrow labeled A indicates the threshold of conduction. Arrows labeled B and C mark features arising from the occupation of the upper-valley and upper confinement subbands, respectively. Under in-plane magnetic field, B evolves into D and E while C evolves into F and G due to spin splitting. The lines at $V_F=2$ V in all the figures are experimental artifacts.

layer, which acts as a back-gate (BG) oxide, was formed by oxygen ion implantation and high-temperature annealing. The top SiO_2 layer acting as a front-gate (FG) oxide was formed by standard thermal oxidation. The nominal thicknesses of the undoped active Si layer, BOX, and top SiO_2 were 10, 380, and 74 nm, respectively. Our sample was fabricated into a Hall-bar geometry with n -type contacts degenerately doped with phosphorus. Standard four-terminal ac lock-in measurements were performed using a source-drain voltage of 10 mV at 13 Hz.

The conductivity σ_{xx} was measured at a temperature of 1.5 K as a function of FG voltage V_F [upper plot of Fig. 2(a)]. Since the position of the features and the background conductivity vary a great deal with BG voltage V_B , we use the double differential $d^2\sigma_{xx}/dV_F^2$ and construct a grayscale plot to highlight the evolution of the features [lower plot of Figs. 2(a) and 2(b)]. As found in previous work on similar devices,¹⁰ feature A represents the threshold of conduction at the mobility edge while features B and C are due to the onset of the occupation of upper subbands. A combination of localization in the upper subband edge and intersubband scattering causes a reduction in the overall mobility when an upper subband begins to occupy. This in turn leads to features in σ_{xx} .

Feature B in Fig. 2(b) is due to the upper-valley subband. It shows a linear dependence of valley splitting on δn , where $\delta n = n_B - n_F$, which we use to empirically quantify the potential asymmetry of the quantum well, where n_B and n_F

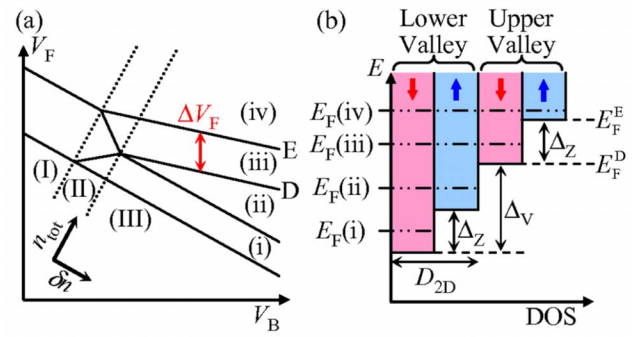


FIG. 3. (Color online) (a) Schematic diagram of subband edges as a function of (V_B, V_F) : $\Delta_V \equiv 0$ (I), $\Delta_Z > \Delta_V$ (II), $\Delta_V > \Delta_Z$ (III). (b) DOS under B_{\parallel} in region (III). Left- and right-hand sides correspond to the DOS of lower- and upper-valleys, respectively. Up and down arrows denote spin up and down states. E_F (i), E_F (ii), E_F (iii) and E_F (iv) correspond to the Fermi energy in regions (i), (ii), (iii), and (iv) in (a). E_F^D and E_F^E correspond to the Fermi energy at D and E, respectively, in Figs. 2(c) and 2(d).

are the electron densities contributed from the BG and FG, respectively. We find that consistent with previous work,¹⁰ the valley splitting can be described by $\Delta_V = \alpha \delta n$, where $\alpha = \text{const}$. The evolution of feature B is best fitted by a value $\alpha = 0.49$ meV/ 10^{15} m⁻² (taking the effective mass to be $m^* = 0.19 m_0$, where m_0 is the free electron mass). This corresponds to a valley splitting of around 10 meV at $\delta n = 2 \times 10^{16}$ m⁻² [red dashed line in Fig. 2(b)]. The region between peaks A and B in Figs. 2(a) and 2(b) corresponds to the valley-polarized regime, where only the lower-valley subband is occupied.

Feature C is due to the upper confinement subband as confirmed by its obeying the expected evolution with V_F and V_B .¹² The valley splitting of this confinement subband is small and is not seen in these measurements because its wave function is never pressed close to the Si BOX interface [Fig. 1(d)].

Figures 2(c) and 2(d) show data taken under identical conditions except for a large in-plane magnetic field of 15 T. In these figures, while the magnetic field enhances localization around A and acts only to shift feature A to higher density,⁹ it is clearly seen that the feature corresponding to the upper-valley subband (B) splits into two as marked by arrows labeled D and E. We interpret this to be due to spin splitting [Fig. 1(e)].

Since B_{\parallel} couples not with the in-plane motion of the electrons but with the spin degree of freedom, we assume a model of the density of states (DOS) with only valley and Zeeman splittings to explain these features. From the model, zones of (V_B, V_F) in Fig. 2(d) can be classified into three, according to the relative magnitudes of Δ_V and $\Delta_Z = g^* \mu_B B$: (I) $\Delta_V \equiv 0$, (II) $\Delta_Z > \Delta_V > 0$, and (III) $\Delta_V > \Delta_Z$, as schematically depicted in Fig. 3(a), where Δ_Z is the Zeeman splitting, g^* is the effective g -factor, and μ_B is the Bohr magneton. A diagram of the DOS for (III) is shown in Fig. 3(b), where the positions of the Fermi energy E_F marked by (i)–(iv) correspond to the regions marked in Fig. 3(a). The DOS of valley and Zeeman split subbands is $D_{2D}/2$, where $D_{2D} = m^*/\pi\hbar^2$. If m^* and g^* are constant, the lines separating regions (i)–(iv) can be expressed analytically by linear equations as functions of V_B and V_F .

We obtain g^*m^* from the separation of the spin split peaks D and E [Fig. 2], $\Delta V_F \equiv V_F^E - V_F^D$, where V_F^D and V_F^E are

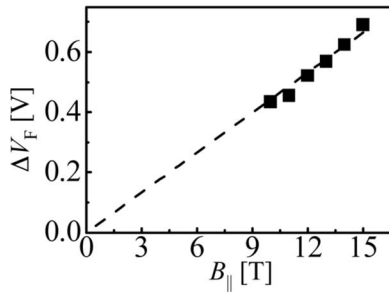


FIG. 4. $B_{||}$ dependence of ΔV_F using data taken at 0.3 K, $V_B=27$ V. The dashed line shows a fit using Eq. (2) giving $g^*m^*=0.49m_0$.

the FG voltages at peaks D and E, and correspond to conditions where the Fermi energy is at E_F^D and E_F^E in Fig. 3(b), respectively. The increment of electron density required in order to increase the Fermi energy from E_F^D to E_F^E is

$$\begin{aligned} \Delta n &= n(E_F = E_F^E) - n(E_F = E_F^D) \\ &= D_{2D}(\Delta_V^E + \Delta_Z) - \frac{D_{2D}}{2}(2\Delta_V^D - \Delta_Z), \end{aligned} \quad (1)$$

where Δ_V^D and Δ_V^E are the valley splittings at D and E respectively. Since ΔV_F can be written as $e\Delta n = C_F \Delta V_F$, ΔV_F is given by

$$\Delta V_F = \frac{3}{2} \frac{eD_{2D}\Delta_Z}{C_F(1 + D_{2D}\alpha)} = \frac{3}{2} \frac{eg^*m^*\mu_B B_{||}}{\pi\hbar^2 C_F(1 + D_{2D}\alpha)}, \quad (2)$$

where C_F is the capacitance between the FG and the 2D electrons. Since parameters C_F and $D_{2D}\alpha$ are determined from SdH oscillations under perpendicular magnetic field¹⁰ and are constants ($462 \mu\text{F}/\text{m}^2$ and 0.39, respectively), g^*m^* is the only variable.

Note that the separation between the peaks is used instead of the peak positions themselves in order to minimize the ambiguity accompanying the position of the actual subband edge in relation to the feature in the conductivity. The similar appearance of both spin subband edges in Fig. 2(d) suggests that the relative separation between the two peaks in the double differential represents the separation of the two subbands with respect to electron occupation.

Figure 4 shows ΔV_F extracted from the data at different values of magnetic field at $V_B=27$ V. The dashed line shows a fit using Eq. (2) giving $g^*m^*=0.49m_0$. Applying the same process to data between $V_B=20$ V and $V_B=40$ V gives

similar values as expected from the parallelism of peaks D and E in Fig. 2(d). The independence of g^*m^* from V_B means that this spin splitting is independent of the amplitude of the valley splitting, total electron density, and potential bias.

The values of the g -factor and effective mass in bulk Si are found to be about 2 and $0.19m_0$, respectively. In dilute systems, it has been reported that g^*m^* increases with decreasing electron density, even in our measured electron-density range (from 3.5×10^{15} to $1.5 \times 10^{16} \text{ m}^{-2}$).^{9,13,14} Although our value does not have an electron-density dependence, it is enhanced compared with the bulk value, as found in previous work.

Finally, we point out that this effect showing spin splitting is not restricted to the upper-valley subband. In Fig. 2(d), the two peaks marked by F and G are consistent with the expected spin splitting of the upper confinement subband edge, demonstrating the generality of this effect. We anticipate that this method can be used to analyze spin-dependent phenomena in a wide range of multisubband systems consisting of other materials as well, by direct transport measurements without complications related to the application of a perpendicular magnetic field.

- ¹S. V. Kravchenko and M. P. Sarachik, *Rep. Prog. Phys.* **67**, 1 (2004).
- ²X. G. Feng, D. Popović, and S. Washburn, *Phys. Rev. Lett.* **83**, 368 (1999).
- ³J. Nitta, T. Akazaki, and H. Takayanagi, *Phys. Rev. Lett.* **78**, 1335 (1997).
- ⁴Y. Tokura, W. G. van der Wiel, T. Obata, and S. Tarucha, *Phys. Rev. Lett.* **96**, 047202 (2006).
- ⁵F. H. L. Koppens, J. A. Folk, J. M. Elzerman, R. Hanson, L. H. Willems van Beveren, I. T. Vink, H. P. Tranitz, W. Wegscheider, L. P. Kouwenhoven, and L. M. K. Vandersypen, *Science* **309**, 1346 (2005).
- ⁶F. F. Fang and P. J. Stiles, *Phys. Rev.* **174**, 823 (1968).
- ⁷V. S. Khrapai, A. A. Shashkin, and V. T. Dolgoplov, *Phys. Rev. Lett.* **91**, 126404 (2003).
- ⁸K. Takashina, M. Brun, T. Ota, D. K. Maude, A. Fujiwara, Y. Ono, Y. Takahashi, and Y. Hirayama, *Phys. Rev. Lett.* **99**, 036803 (2007).
- ⁹T. Okamoto, K. Hosoya, S. Kawaji, and A. Yagi, *Phys. Rev. Lett.* **82**, 3875 (1999).
- ¹⁰K. Takashina, Y. Ono, A. Fujiwara, Y. Takahashi, and Y. Hirayama, *Phys. Rev. Lett.* **96**, 236801 (2006).
- ¹¹M. A. Wilde, M. Rhode, Ch. Heyn, D. Heitmann, D. Grundler, U. Zeitler, F. Schäffler, and R. J. Haug, *Phys. Rev. B* **72**, 165429 (2005).
- ¹²K. Takashina, Y. Ono, A. Fujiwara, Y. Takahashi, and Y. Hirayama, *IEEE Trans. Nanotechnol.* **5**, 430 (2006).
- ¹³A. A. Shashkin, S. V. Kravchenko, V. T. Dolgoplov, and T. M. Klapwijk, *Phys. Rev. Lett.* **87**, 086801 (2001).
- ¹⁴V. M. Pudalov, M. E. Gershenson, H. Kojima, N. Butch, E. M. Dizhur, G. Brunthaler, A. Prinz, and G. Bauer, *Phys. Rev. Lett.* **88**, 196404 (2002).